Journal of Aeronautical and Automotive Engineering (JAAE)
Print ISSN: 2393-8579; Online ISSN: 2393-8587; Volume 2, Number 1; January-March, 2015 pp. 50-54

http://www.krishisanskriti.org/jaae.html

Vibrational Analysis of Ornithopter

A.M. Anushree Kirthika

Dept.of Aeronautical Engineering, Rajalakshmi Engineering College, Thandalam, Tamilnadu, India
E-mail: anushreekirthika.am.2011.aero@ rajalakshmi.edu.in

Abstract—*The ornithopter when constrained to one dimensional horizontal motion , a simplified model is said to be derived in accordance to mass with damping subject to a forcing input. The study of one dimensional horizontal model of ornithopter with disturbance and the controllability of such system is carried out. The transfer function of the model is assumed to be a step input where the step input is the DC component of acceleration. A study is made on the basis of separation of DC and Non DC components.*

Keyword: *One dimensional horizontal model , control*

1. INTRODUCTION

An ornithopter is an aircraft that uses flapping wing motion to fly. This type of flight offers potential advantages over fixed-wing flight, such as maneuverability at slow speeds (1-40m/s). Natural ornithopters range in size from small flying insects to large birds and flap their wings from about 5 to 200Hz. The controllability of systems subjected to vibrational, periodic, and oscillatory inputs through averaging analyses and evidence of superior low-speed flight capability with flapping flight are studied to control the ornithopter. We get a brief knowledge of Analyze motion data of an ornithopter MAV in order to develop a system transfer function to examine the frequency spectrum of the forcing input created by an ornithopter's flapping wings and Characterize and model the forcing input created by the wings.

2. BASIC EQUATIONS INVOLVED IN ORNITHOPTER FOR ONE DIMENSIONAL HORIZONTAL MOTION

This study describes the data analysis and modeling of the ornithopter. First, a basic model of the ornithopter is derived using equations of motion. Then, the net force driving the ornithopter is characterized based on the acceleration data. Work is then done to find a specific transfer function of the ornithopter based on the basic model and motion data.

Basic Model

In the case of the ornithoper constrained to one-dimensional horizontal motion, a simplified model can be expressed as a mass with damping subject to a forcing input. The following equation of motion describes the time-domain model of the ornithopter, which is pictured in Fig. 1:

$f(t) = m\ddot{x} + B\dot{x} = m\dot{\upsilon} + B\upsilon$

From this equation, a transfer function from forcing input to velocity output can be obtained through a Laplace Transform as:

$F(s) = msV(s) + BV(s) = (ms + B)V(s)$.

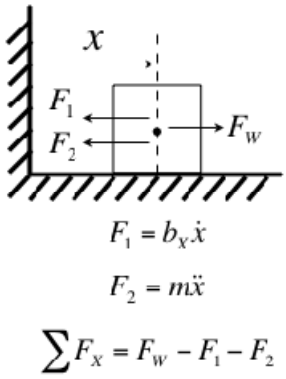

Fig. 1: One-Dimensional Free Body Diagram of Ornithopter: Horizontal Movement

Giving the transfer function:

$$P(s) = \frac{V(s)}{F(s)} = \frac{1}{ms + B} = \frac{1/m}{s + B/m}$$

We can also obtain the transfer function from acceleration to velocity as:

$$\frac{V(s)}{F(s)} = \frac{V(s)}{mA(s)} = \frac{1/m}{s + B/m}$$

$$\frac{V(s)}{A(s)} = mP(s) = \frac{1}{s + B/m} \qquad (2.1)$$

Thus, a first-order transfer function from acceleration input to velocity output can be determined to match the gain and rise-time of the measured velocities. However, the acceleration must first be characterized in order to simulate it as an input to the transfer function, if the simulation is required.

Frequency Analysis and Simulation of Acceleration

The frequency spectrum of the filtered acceleration data, shown in Figure.2, reveals some important things about the system under study. The frequency of flapping (or forcing) is determined to be the smallest non-DC frequency component of the acceleration. Table 2.1 summarizes the estimated flapping frequency found at each throttle. These values change slightly, by about ±0.1Hz, depending on the period of the data examined. Each acceleration signal can be summarized through a Fourier series expansion, as:

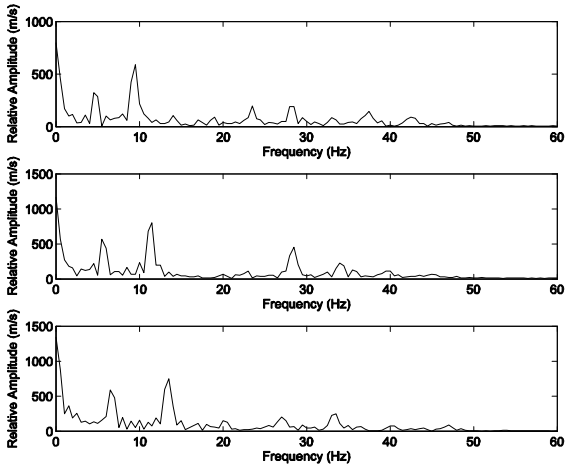

Fig. 2: Frequency Spectrum of Filtered Acceleration Data

Table 2.1: Throttle vs. Estimated Frequency of Flapping

Throttle	Frequency of Flapping
1/4	4.6 Hz
1/2	5.6 Hz
3/4	6.6 Hz

$$a(t) = \sum_{i=0}^{n} \left\{ M_i \cos\left(w_i t + \varphi_i\right) \right\} = \text{fourier series} \qquad (2.2)$$

Where n is the number of components (or harmonics) used to represent the signal. In this way, the acceleration can be simulated using the frequency, amplitude, and phase of the most prominent components. For instance, Table 2.2 summarizes this information for the five most prominent components of the acceleration at 1/2 throttle. Each acceleration signal is cut to one representative period in order to allow for simulation over an unspecified amount of time and to avoid windowing problems. Windowing problems occur when frequency components exist which correspond to the period of the

window of time in which the data is taken. Because data is available for three different throttles, a third-order polynomial can be fit to the three Fourier series expansions to approximate acceleration at other throttles. Also, to avoid the ambiguity of approximate "throttle," the estimated frequency of flapping is used instead as the input.

Table 2.2 : Summary of Amplitude, Frequency, and Phase of the Five Most Prominent Components in Acceleration at 1/2 Throttle

Component	1	2	3	4	5
Relative Amplitude (m/s)	594.2	230.9	511.1	25.0	25.0
Frequency (hertz)	0	5.6	11.3	16.9	22.5
Phase (radians)	0	1.7	2.9	2.4	-2.0

In addition to limiting the input range, the acceleration is modified to account for slowly time-varying inputs. This allows one to change the frequency of flapping during simulation without incongruities in the acceleration. This can be done by incorporating changes in frequency into the phase, since phase is the time integral of frequency. In this case one component of the acceleration signal is expressed as:

$$S_{n+1} = A_{n+1}\cos(\phi_{n+1})$$

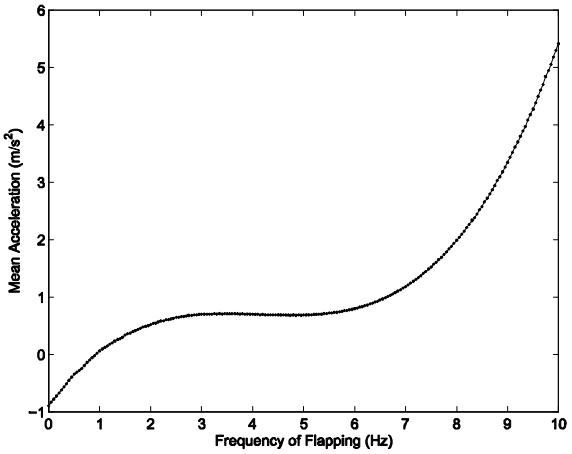

Fig. 3. Frequency of Flapping vs. Simulated Mean Acceleration

Model Assumptions and Corrections

While verifying the model transfer function in the previous section, the acceleration input is assumed to be a step input where the magnitude of the step is the DC component of the

acceleration. This assumption is verified by separating the DC and non-DC components of the acceleration and viewing the non-DC components as a disturbance to the system:

$$A(t) = \sum_{i=0}^{n} \left\{ M_i \cos\left(\omega_i t + \varphi_i\right) \right\} \quad (2.3)$$

$$= M_0 + \sum_{i=1}^{n} M_i \left\{ \frac{s * \cos\left(\varphi_i\right) - \omega_1 * \sin\left(\varphi_i\right)}{s^2 + \omega_i^2} \right\} \quad (2.4)$$

A model of the ornithopter with transfer function from acceleration to velocity and from forcing to velocity is shown in Fig. 4. Here, the input $u(s) = \frac{M_0}{s}$ and the disturbance

$$d(s) = \sum_{i=1}^{n} M_i \left\{ \frac{s * \cos(\varphi_i) - \omega_i * \sin(\varphi_i)}{s^2 + \omega_i^2} \right\} \quad (2.5)$$

In an ideal case each sinusoidal term is symmetric about zero and each will have a net effect in acceleration of zero over time. Since we are

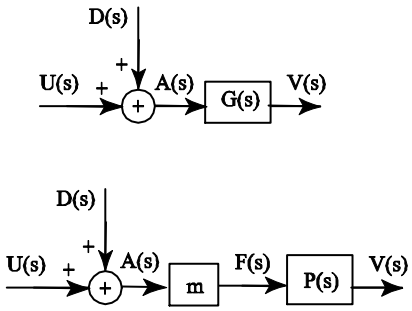

Fig. 4: One-Dimensional Horizontal Model of Ornithopter with Disturbance

assuming a linear model of the ornithopter, the velocity output from each pure sinusoidal input term will include a magnitude and phase change, but will still be symmetric about zero. As we do not have an ideal case and the ornithopter is not completely linear, some error in the velocity output is expected to exist.

As the modeling done in the previous sections has been concerned with the experimental data, it reflects the motion of the total mass of the ornithopter and slider used to attach it to the linear bearing rail. If we assume that the same force is generated by the ornithopter with and without the mass of the slider included, we can make the following calculations for the ornithopter's actual acceleration:

$F = ma$

$M_{test} a_{test} = m_{ornithopter} a_{new}$

$$a_{new} = \frac{m_{test}}{m_{test}} a_{test} = \frac{0.2\,\text{kg}}{0.096\,\text{kg}} a_{test}$$

$$a_{new} \approx 2 a_{test}$$

Therefore, the acceleration of the ornithopter alone is twice that of the sensor data acceleration.

One-Dimensional Horizontal Closed-Loop System

The following sections address challenges created by flapping of the wings, controllability and stability of the one-dimensional ornithopter model, and design of a controller.

Feedback Path Filter

A filter is used in the feedback path of the closed-loop system to avoid tracking of fluctuations in velocity created by the flapping of the wings. Though the ornithopter itself acts as a low pass filter (LPF), which filters the forcing input and has a cut off frequency at about 1rad/sec fluctuations still exist in the velocity as it is evident upon examination of the velocity data. This is problematic as the frequency of flapping is close to that of the oscillations, one might see in velocity about steady-state. A LPF can be used to eliminate the majority of the unwanted frequency components and to facilitate tracking of the mean velocity. A LPF of the following form was chosen:

$$H(s) = \frac{a}{s + a}$$

For $a < 0$.

In choosing the placement of the filter pole one must consider the trade off between the delay of the filter and its filtering capability. As the filter pole decreases in magnitude, the filtering capability of lower frequencies increases. Because the contribution of the filtered frequency components is attenuated, the magnitude of the filtered signal is smaller and takes longer to reach a steady-state value. This is seen as a delay in the filter output and so it takes longer to track the actual velocity. A unity gain filter with good filtering capability limited delay was chosen to filter frequencies above 0.5 Hz:

$$H(s) = \frac{2\pi * 0.5}{s + (2\pi * 0.5)} = \frac{\pi}{s + \pi}$$

3. THE FLAPPING-FEATHERING MECHANISM

This study is said to be made with respectively analysis of mechanism in a typical pigeon (Columba livia).

The flapping motion of the wing is described by a planar four-bar mechanical linkage, while the feathering motion is described by a modified five-bar linkage that can be highly approximated by an equivalent planar four-bar mechanical linkage in the synthesis. These two mechanical linkages are interconnected to form a set of flapping-feathering mechanism to produce a properly coordinated flapping and feathering motion of the wing for an entire flapping cycle. The insertion of joint C in the feathering mechanism allows the links EC and O_4C to have an additional degree of freedom in a moving plane to determine the position of the link O_4B of the flapping mechanism that eventually allows the smooth motion of the two interconnected mechanisms. The flapping-feathering mechanism has been designed to have the same upstroke and down stroke period throughout the entire flapping cycle for a constant crank (O_2A) angular speed input.

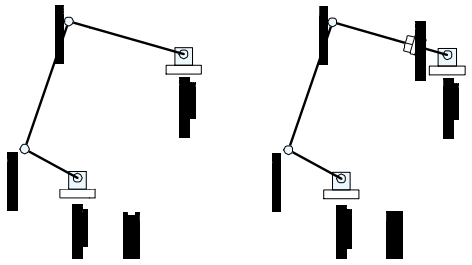

Fig. 5 (a) The flapping, and 5(b) feathering mechanisms.

Velocity :

$$\begin{bmatrix} -r_3 \sin\theta_3 & r_4 \sin\theta_4 \\ -r_3 \cos_3 & r_4 \cos\theta_4 \end{bmatrix} \begin{Bmatrix} \theta_3 \\ \theta_4 \end{Bmatrix} = \begin{Bmatrix} r_2\,\theta_2 \sin\theta_2 \\ r_2\,\theta_2 \cos\theta_2 \end{Bmatrix} \tag{3.1}$$

$$\vec{r}\,p = r_4\,\theta_4\left(-\sin\theta_2\,i + \cos\theta_2 j\right)$$

$$\vec{r}\,p = r_4\,\theta_4\left(-\sin\theta_4\,i + \cos\theta_4 j\right) \tag{3.2}$$

Acceleration:

$$\begin{bmatrix} -r_3 \sin\theta_3 & r_4 \sin\theta_4 \\ -r_3 \cos_3 & r_4 \cos\theta_4 \end{bmatrix} \begin{Bmatrix} \theta_3 \\ \theta_4 \end{Bmatrix} =$$

$$\begin{Bmatrix} r_2\,\theta_2 \sin\theta_2 + r_2\,\theta_2^2 \cos\theta_2 + r_3\,\theta_3^2 \cos\theta_3 - r_4\theta_4^2 \cos\theta_4 \\ r_2\,\theta_2 \cos\theta_2 + r_2\,\theta_2^2 \sin\theta_2 + r_3\,\theta_3^2 \sin\theta_3 - r_4\theta_4^2 \sin\theta_4 \end{Bmatrix} \tag{3.3}$$

$$\vec{r}_2 = \left(-r_2\,\theta_2 \sin\theta_2 - r_2\,\theta_2^2 \cos\theta_2\right)i + \left(r_2\,\theta_2 \cos\theta_2 - r_2\,\theta_2^2 \sin\theta_2\right)j \tag{3.4}$$

$$\vec{r}_p = \left(-r_4\,\theta_4 \sin\theta_4 - r_4\,\theta_4^2 \cos\theta_4\right)i + \left(r_4\,\theta_4 \cos\theta_4 - r_4\,\theta_4^2 \sin\theta_4\right)j \tag{3.5}$$

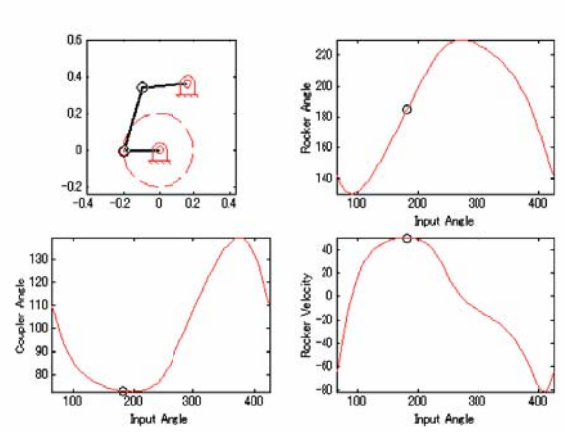

Fig. 6: Plot of the flapping wing kinematics

4. CONTROL METHOD

Autonomous flight control of the ornithopter is implemented with the onboard sensors and microprocessor described in Section II. The desired angle and the orientation angle are fed into the regulator, shown in Fig 7. consisting of two PID controllers running at 400 Hz. The PID controllers compute the input signals (two PWM signals) to drive the wings and the propeller. For the PID controllers, we assume that the propeller mainly contributes the yaw moment and the wings mainly contribute pitch moment and thrust.

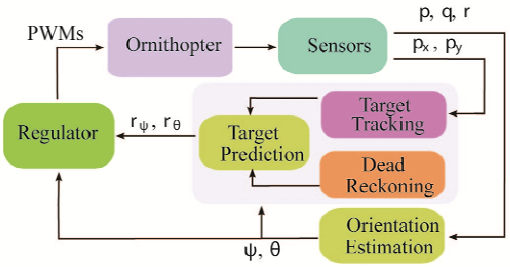

Fig. 7: Block diagram for the PID controllers

The input signals for the ornithopter thrust from the wings and steering moment from the propeller are computed based on the PID controller given by,

$$u = k_p(r - y) + k_i \int_0^t (r(\tau) - y(\tau))d\tau + k_d \left(\gamma \dot{r} - \dot{y}\right),$$

where *u* is the duty cycle for a motor, *kp*, *ki*, and *kd* are, respectively, proportional, integral, and derivative gains for the PID controller, *r* is the desired angle, *y* is the measured orientation angle, and γ is the reference weight for the derivative controller. We set $\gamma = 0$ to avoid large transients in the control signal when the reference is changed. Setting $\gamma = 0$ also allows us to relocate the poles at zero to the left half plane. There are two such PID controllers running simultaneously for yaw and pitch regulation. A third order Butterworth low pass filter is implemented to reduce high frequency noise for $\dot{y}$. A discrete time anti-windup algorithm is also implemented by testing if the actuator is saturated; the PWM duty cycle to the motors, denoted by *u*, should stay between *vmin* and *vmax*, where *v* is the input to the plant. If the actuator is not saturated, i.e., $vmin < u < vmax$, we accumulate the errors for the integral controller. If the actuator is saturated, the accumulated errors remain unchanged. The controller algorithm discussed here is summarized in Figure.8.

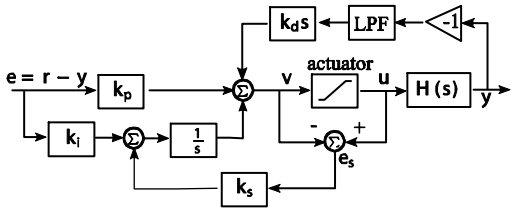

Fig. 8: Plot of the flapping wing kinematics

5. CONCLUSION

Thus the study and analysis of ornithopter when subjected to one dimensional horizontal motion has been done. The controllability of a flapping wing MAV with wings limited to a single degree of freedom is studied and analyzed by usage of average and high frequency control. Control of ornithopter was said to be done by the method of usage of onboard sensor and a microcontroller without any external assistance by the implementation of desired angle along with the orientation angle are fed into the regulator.

The flapping and feathering mechanism that was implemented in flapping wing MAV model for a typical pigeon (Columba livia) was studied in the area of vibrational analysis.

REFERENCE

[1] J.D. DeLaurier, "An aerodynamic model for flapping –wing flight", Journal of The Royal Aeronautical Society, April 1993.

[2] Jonathan Maglasang, Koji Isogai, Norihiro Goto, and Masahide Yamasaki, "Aerodynamic Study and Mechanization Concepts for Flapping – Wing Micro Aerial Vehicels", Journal of Faculty of Engineering Kyushu University, vol.66, No.1, March 2006.

[3] Stanley S. Baek, Fernando L, Garcia Bermudez, and Ronald S. Fearing. "Flight Control for Target Seeking by 13 gram Ornithopter".

[4] Katherine Sarah Shigeoka, "Velocity and Altitude Control of an Ornithopter Micro Aerial Vehicle".

[5] S. Baek and R. Fearing, "Flight forces and altitude regulation of 12 gram I-Bird," in IEEE RAS and EMBS International Conference on Biomedical Robotics and Biomechatronics (BioRob), Tokyo, Japan, September 2010, pp. 454–460.